Comprehensive Analysis of P and S Spectra from Southern California Earthquakes

Award 04HQGR0113

Peter M. Shearer
Institute of Geophysics and Planetary Physics
Scripps Institution of Oceanography
University of California, San Diego
La Jolla, CA 92093
858-534-2260 (phone), 858-534-5332 (fax)
pshearer@ucsd.edu

Key words: Seismology, Seismotectonics, Source Characteristics

Annual Progress Summary Report

Investigations Undertaken

This project involves computation and analysis of *P* and *S* spectra from over 300,000 southern California earthquakes recorded since 1984. Our studies are concerned with the following issues:

• Do earthquake source spectra scale such that apparent stress is constant with respect to event size?

• Do earthquake stress drops in southern California vary systematically in space and time?

• What is the three-dimensional attenuation structure beneath southern California?

• Can directivity effects be routinely observed in earthquake source spectra?

• Can *P* and *S* amplitude information help improve earthquake focal mechanism accuracy compared to *P* polarity information alone?

Anticipated results of this work include a more detailed understanding of earthquake source properties and new maps of lateral variations in crustal attenuation. This knowledge will contribute to quantitative assessments of earthquake potential and seismic hazard in southern California.

Results

Computing P and S spectra

We have completed the necessary software to compute spectra from our online waveform database and have obtained spectra from over 300,000 events. This involved selecting windows around both the *P* and *S* waves, using the operator phase picks, if available, or applying an automatic picking algorithm. Spectra are currently computed using a multitaper method from all available channels and components, including rotation into transverse and radial components. Spectra are also computed from pre-arrival noise windows in order to estimate signal-to-noise ratios (Figure 1). We store the spectra in a special binary format designed for rapid storage and retrieval of the millions of spectra we obtain. Our spectral database currently requires about 60 Gbytes of storage on a RAID system at Caltech.

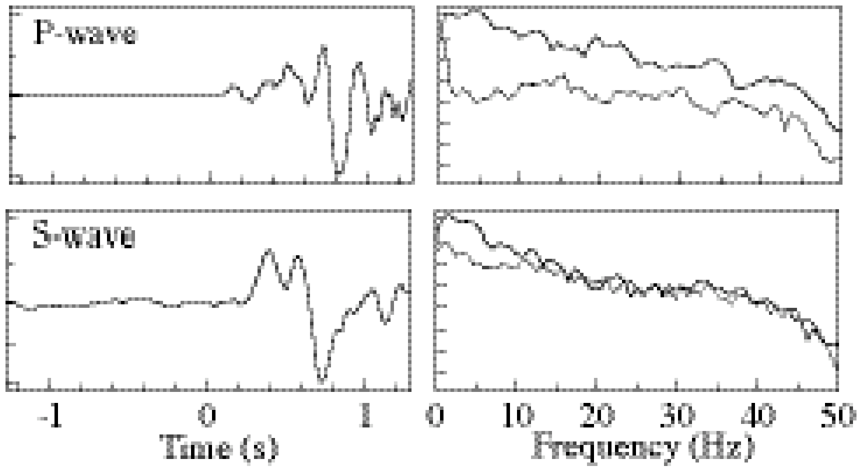

Figure 1. Windowed time series and spectra for a M = 5.4 earthquake (22 Feb. 2003) near Big Bear recorded by station ADO at 60 km distance, as computed with our automatic algorithm. Noise and signal spectra are computed using 1.28 s windows immediately before and after the phase arrival. Signal spectra are plotted as thick lines, noise spectra as thin lines. The *P* wave has much better signal-to-noise at high frequencies than the *S* wave.

Processing the spectra

Following application of a signal-to-noise cutoff criteria and corrections for the known gain and instrument response, we process the spectra in ways that isolate source, receiver and propagation path effects. This is an important step because individual spectra tend to be noisy and irregular in shape and difficult to fit robustly with theoretical models. However, by stacking thousands of spectra it is possible to obtain much more consistent results.

Following Warren and Shearer (2000, 2002), the basic approach is to assume that each observed spectrum $D_{ij}(f)$ from source i and receiver j is a product of source effects S_i (which include the source spectrum and near-source attenuation), near-receiver effects R_j (which includes any uncorrected part of the instrument response, the site response and the near-receiver attenuation), an along-path attenuation operator A_{ij}, and a frequency-independent operator G_{ij} that includes geometrical spreading:

$$D_{ij}(f) = S_i(f)\ A_{ij}(f)\ R_j(f)\ G_{ij}$$

Because each station records multiple events and each event is recorded by multiple stations, this is an over-determined problem for the source and station terms. We solve for these terms through an iterative procedure that stacks the spectra to obtain source- and receiver-specific spectra. Note that this method resolves only differences in the relative shapes of the spectra. Without additional modeling assumptions, it cannot, for example, resolve how much of the spectral falloff is due to source effects and how much is due to attenuation common to all paths. The advantage of the method, however, is that it identifies and removes anomalies that are specific to certain sources or receivers. Because there may be difficulties in obtaining reliable and accurate instrument response functions for many of the stations in the archive, this is an important processing step that provides a way to correct for some of these problems.

Results of preliminary t analysis*

Fully implementing the above stacking procedure for our complete database will require some effort because the number of spectra involved is too large to fit into computer memory. However, the same approach can be applied to t^* measurements obtained from individual spectra. We have computed t^* from over 2 million individual *P*-wave spectra with average signal-to-noise ratios of 5 or better between 1989 and 2003 by fitting over the 5 to 15 Hz band, after first correcting the records to displacement. We process these t^* values by iteratively averaging to obtain source and receiver terms, as well as empirical corrections for event size, event depth, and source-receiver distance. Our observed distance dependence of t^* between 0 and 160 km is consistent with a mid-crustal Q_P of about 500, in approximate agreement with Schlotterbeck and Abers (2001).

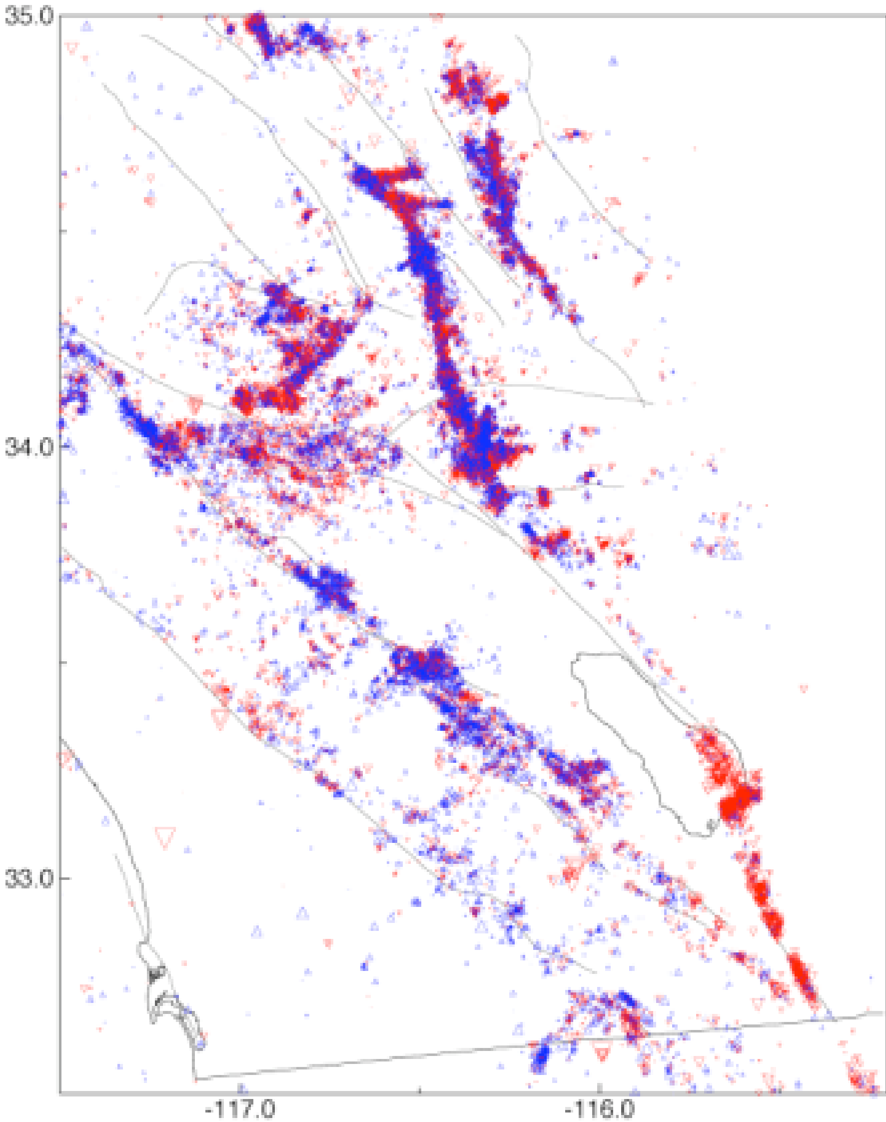

Figure 2. Source variations in apparent t^* values for 49,340 earthquakes from 1989 to 2003, plotted after removing empirical corrections for magnitude, station response, and average attenuation. Symbol size is proportional to the magnitude of t^* with red indicating higher than average t^* and blue indicating lower than average t^*. Plotted values range from about ±0.05 s.

The most intriguing result of this analysis is the variability in the source t^* terms as illustrated in Figure 2. Larger than average t^* values (reduced high frequencies) are plotted in red and smaller than average t^* values (increased high frequencies) are plotted in blue. These source terms exhibit spatially coherent patterns. For example, events in the Imperial Valley are relatively depleted in high frequencies, indicating either low-corner-frequency, low-stress-drop (slow) events or large near-source attenuation. We prefer the former explanation because seismic stations in this region do not exhibit anomalous t^* values, but fully discriminating between these effects in this region will require more detailed analysis of the spectral shapes and possible implementation of an empirical Green's function (EGF) approach. However, rapid t^* variations shown in other parts of Figure 2 are almost certainly caused by variations in source properties because the required changes in Q_P at short distances would be unrealistically large. For example, aftershocks of the 1992 Landers rupture exhibit along strike variations in their frequency content that suggest variations in corner frequencies and stress drops along the fault. Comparisons of these results to focal mechanisms and static stress change predictions from Landers rupture models should improve our understanding of how aftershocks respond to stress changes.

Earthquake source scaling

P and *S* spectra provide fundamental constraints on earthquake source properties. Some important parameters are the moment (estimated from the long-period displacement spectrum), the stress drop (derived from the observed corner frequency), and the apparent stress (derived from the integrated velocity spectrum). These parameters play a key role in the current debate over whether earthquakes are self-similar over a wide range of event size. Self-similarity would imply that stress drop and apparent stress should be constant as a function of moment. Several authors find evidence that apparent stress increases with magnitude (e.g., Kanamori et al., 1983; Abercrombie, 1995; Mayeda and Walter, 1996; Izutani and Kanamori, 2001) while others argue that apparent stress is approximately constant (e.g., Choy and Boatwright, 1995; McGarr, 1999; Ide and Beroza, 2001).

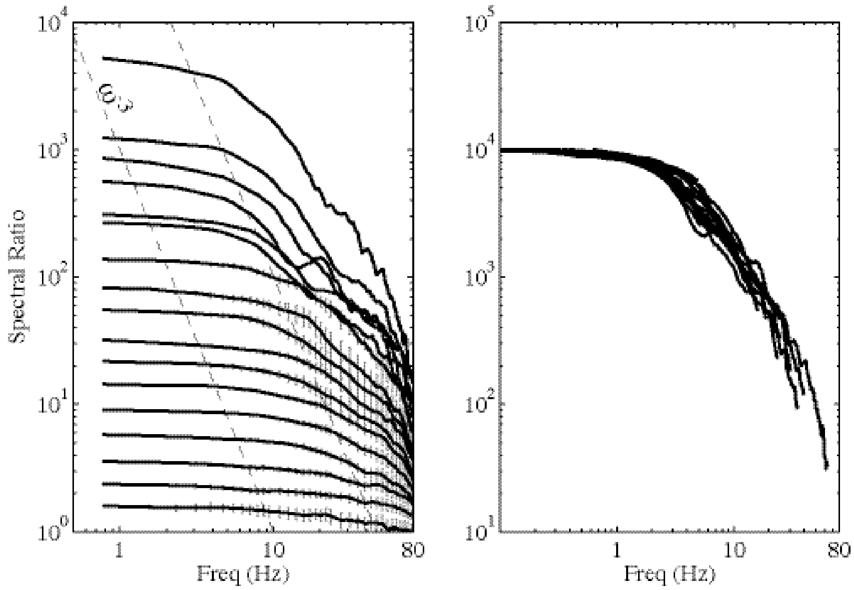

Figure 3. EGF corrected stacked *S*-wave spectra from a cluster of events recorded by the Anza Seismic Network for bins of different source moment, showing the self-similarity of the spectra when shifted along an ω^{-3} line. As shown to the right, the spectral shapes agree within their estimated uncertainties.

Given the large scatter in observed values of stress drop and apparent stress, even at constant event moment, this is a difficult issue to resolve. To observe a significant trend in stress as a function of moment, a wide range of event sizes must be studied. Reliably estimating total radiated seismic energy for large events has proven problematic, with teleseismic and regional estimates of energy for the same earthquake often showing large differences. Obtaining results for small earthquakes (M < 3) requires measurements extending to high frequencies where corrections for attenuation become critical. In some cases, band-width limitations and/or event selection bias may significantly affect the results (Ide and Beroza, 2001).

Some of these difficulties could be reduced if spectra from large and small earthquakes were compared directly, rather than comparing properties derived from the spectra, such as corner frequency and integrated energy. Since individual spectra are typically irregular in detail (i.e., they don't fit simple theoretical models), such comparisons are probably best performed on stacks of many events. We have successfully applied this approach to a cluster of ~400 earthquakes recorded by the Anza seismic network (Prieto et al., 2004). Figure 3 plots EGF-corrected *S*-wave spectra, stacked in bins of similar moment. Over the M = 1.5 to 3.2 range of the data, the spectra are the same shape when shifted along the ω^{-3} line predicted by self-similarity. Apparent stresses computed from these spectra are almost constant with respect to moment, again consistent with the self-similarity hypothesis. Figure 4 shows our results compared to other studies, as summarized by Ide and Beroza (2001).

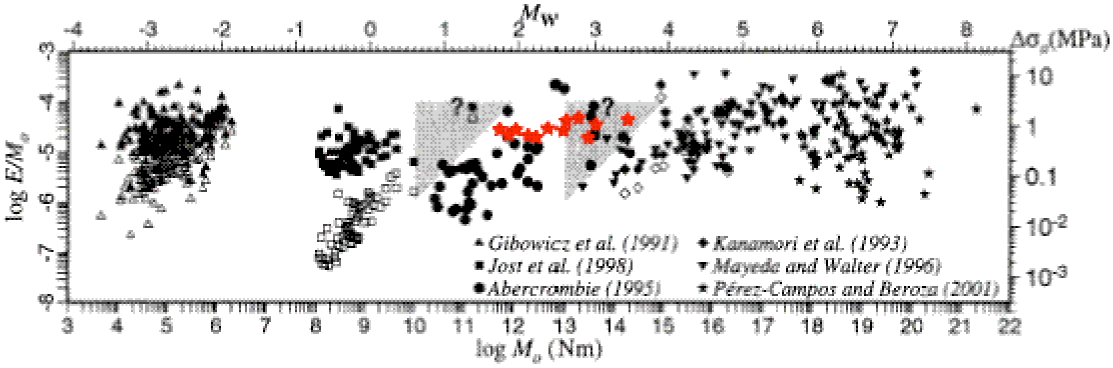

Figure 4. Observed apparent stress as a function of moment from different studies, as plotted by Ide and Beroza (2001). Our new results for the Anza earthquake cluster are shown in red stars. They generally lie above previous results by Abercombie (1995) and support models of constant apparent stress.

References

Abercrombie, R.E., Earthquake source scaling relationships from –1 to 5 ML using seismograms recorded at 2.5-km depth, *J. Geophys Res.*, **100**, 24,015-24,036, 1995.

Choy, G.L. and J.L. Boatwright, Global patterns of radiated seismic energy and apparent stress, *J. Geophys. Res.*, **100**, 18,205-18,228, 1995.

Ide, S. and G.C. Beroza, Does apparent stress vary with earthquake size?, *Geophys. Res. Lett.*, **28**, 3349-3352, 2001.

Izutani, Y. and H. Kanamori, Scale-dependence of seismic energy-to-moment ratio for strike-slip earthquakes in Japan, *Geophys. Res. Lett.*, **28**, 4007-4010, 2001.

Kanamori, H., E. Hauksson, L.K. Hutton, and L.M. Jones, Determination of earthquake energy release and Ml using TERRAscope, *Bull. Seismol. Soc. Am.*, **83**, 330-346, 1993.

Mayada, K. and W.R. Walter, Moment, energy, stress drop, and source spectra of western United States earthquakes from regional coda envelopes, *J. Geophys Res.*, **101**, 11,195-11,208, 1996.

McGarr, A., On relating apparent stress to the stress causing earthquake slip, *J. Geophys. Res.*, **104**, 3003-3011, 1999.

Prieto, G., P.M. Shearer, F.L. Vernon and D. Kilb, Earthquake source scaling and self-similarity estimation from stacking P and S spectra, *J. Geophys. Res.*, 109, B08310, doi:10.1029/2004JB003084, 2004.

Schlotterbeck, B.A. and G.A. Abers, Three-dimensional attenuation variations in southern California, *J. Geophys Res.*, **106**, 30,719-30,735, 2001.

Warren, L.M. and P.M. Shearer, Investigating the frequency dependence of mantle Q by stacking P and PP spectra, *J. Geophys Res.*, **105**, 25,391-25,402, 2000.

Warren, L.M and P.M. Shearer, Mapping lateral variations in upper mantle attenuation by stacking *P* and *PP* spectra, *J. Geophys Res.*, **107**(B12), 2342, doi: 10.1029/2001JB001195, 2002.

Non-technical Summary

Seismic wave spectra provide valuable information about earthquake source properties and the attenuation structure of the southern California crust. We systematically compute compressional and shear-wave spectra from over 300,000 southern Californian earthquakes and analyze them to separate source and propagation path effects.

Reports Published

Grant, L.B. and P.M. Shearer, Activity of the offshore Newport-Inglewood Rose Canyon fault zone, coastal southern California, from relocated microseismicity, *Bull. Seismol. Soc. Am.*, 94, 747-752, 2004.

Prieto, G., P.M. Shearer, F.L. Vernon and D. Kilb, Earthquake source scaling and self-similarity estimation from stacking P and S spectra, *J. Geophys. Res.*, 109, B08310, doi:10.1029/2004JB003084, 2004.